European Journal of Chemistry

Journal webpage: www.eurjchem.com

N-(Dibenzylcarbamothioyl)-3-methylbutanamide: Crystal structure, Hirshfeld surfaces and antimicrobial activity

Ilkay Gumus [1,*], Serpil Gonca [2], Birdal Arslan [1], Ebru Keskin [3], Ummuhan Solmaz [1] and Hakan Arslan [1]

[1] *Department of Chemistry, Faculty of Arts and Science, Mersin University, Mersin, TR 33343, Turkey*
[2] *Department of Pharmaceutical Microbiology, Faculty of Pharmacy, Mersin University, Mersin, TR 33343, Turkey*
[3] *Advanced Technology Research and Application Center, Mersin University, Mersin, TR 33343, Turkey*

** Corresponding author at: Department of Chemistry, Faculty of Arts and Science, Mersin University, Mersin, TR 33343, Turkey.*
Tel.: +90.324.3610001/14559. Fax: +90.324.3610047. E-mail address: ilkay.gumus@mersin.edu.tr (I. Gumus).

ARTICLE INFORMATION

DOI: 10.5155/eurjchem.8.4.410-416.1650

Received: 20 October 2017
Received in revised form: 08 November 2017
Accepted: 09 November 2017
Published online: 31 December 2017
Printed: 31 December 2017

KEYWORDS

Thiourea derivative
Antimicrobial activity
Single crystal structure
Molecular self-assembly
Hirshfeld surface analysis
Deformation electron density

ABSTRACT

The compound *N*-(dibenzylcarbamothioyl)-3-methylbutanamide as a thiourea derivative was synthesized and structurally characterized by NMR and FT-IR spectroscopic techniques. The molecular structure of compound was also characterized by single crystal X-ray diffraction method. Crystal data for title compound $C_{20}H_{24}N_2OS$: monoclinic, space group C2/c (no. 15), a = 19.6882(9) Å, b = 9.4045(4) Å, c = 19.5012(8) Å, β = 98.433(2)°, V = 3571.8(3) Å^3, Z = 8, μ(CuKα) = 1.665 mm^{-1}, 25057 reflections measured (9.168° ≤ 2Θ ≤ 144.196°), 3500 unique (R_{int} = 0.0322, R_{sigma} = 0.0200) which were used in all calculations. The final R_1 was 0.0363 (I>2σ(I)) and wR_2 was 0.0910 (all data). Intermolecular contacts obtained from X-ray single crystal diffraction study were also explored using both Hirshfeld surfaces and fingerprint plots. Hirshfeld surface analysis showed the occurrence of S···H, O···H and H···H contacts that display an important role to crystal packing stabilization of the thiourea derivative compound. In addition, the compound was evaluated for both their *in-vitro* antibacterial and antifungal activity.

Cite this: *Eur. J. Chem.* **2017**, *8(4)*, 410-416

1. Introduction

Thiourea species are important organic compounds that act as basic building block for synthesis of heterocyclic compounds [1,2]. They have especially drawn attention with their wide range of biological activities, like bactericidal, fungicidal, herbicidal and insecticidal, and they possess regulating activity for plant growth [3-5]. They also have potantial as anti-cancer agents against various leukemia and solid tumors [6].

N-(Alkyl/aryl)-*N'*-acylthiourea and *N*-di(alkyl/aryl)-*N'*-acylthiourea derivatives, which have oxygen, nitrogen and sulfur donor atoms, act as versatile ligands with various coordination modes. These ligands exhibit prevalent coordination systems such as neutral bidentate and monobasic bridging in some complexes [7-22]. Since the structural and conformational properties of acyl thioureas has been recognized, the use of transition metal complexes, including acylthiourea ligands, have been expanded in many different fields [9-12]. For example, acylthiourea derivatives and their Co(III) complexes have shown antibacterial [13] and antifungal [14] activities. Ni(II) complexes, containing benzoylthiourea ligands, have shown cytotoxicity against T47D cell [15] and according to the investigations water soluble platinum(II) benzoylthiourea complexes have shown considerable antimalarial activity [23,24]. Very recently, there have been many studies on noncovalent interactions acting on the crystal structure and packing of sulfur-containing compounds [25]. Hydrogen bonds are generally dominant in the crystal packing of acyl thiourea compounds, mostly determined to be both, N–H···O=C and N–H···S=C interactions [26,27]. When we looked at the synthesized crystals before, it could be seen that most of the structures displayed a characteristic intermolecular pattern forming dimers by N–H···S hydrogen bonding [7,12].

The success of many applications of acylthioureas are based on the formation of proper hydrogen bonds with particular receptors [28,29]. The main purpose of our study is to understand the structural properties of thiourea derivative compounds. In order to this *N*-(dibenzylcarbamothioyl)-3-methylbutanamide has been synthesized and the effect of intramolecular interactions on conformational properties has been investigated by single crystal X-ray diffraction. Intermolecular contacts obtained from X-ray single crystal diffraction study were also explored using both Hirshfeld surfaces and fingerprint plots.

ISSN 2153-2249 (Print) / ISSN 2153-2257 (Online)
http://dx.doi.org/10.5155/eurjchem.8.4.410-416.1650

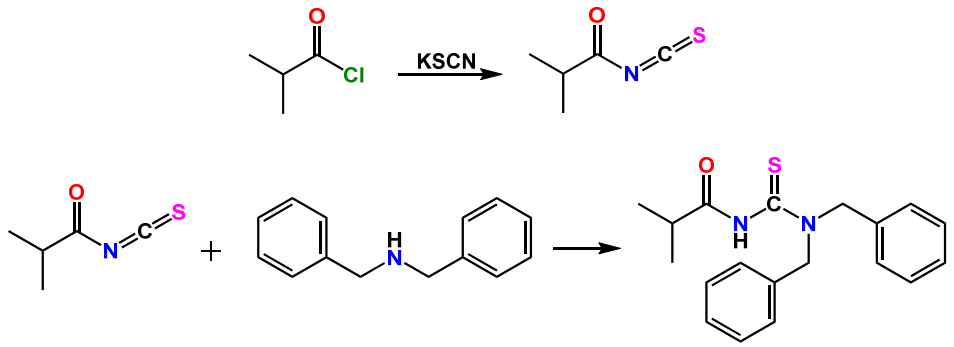

Scheme 1

2. Experimental

2.1. Instrumentation

Infrared measurement was recorded in the range 400-4000 cm^{-1} on a Perkin Elmer Spectrum 100 series FT-IR/FIR/NIR Spectrometer Frontier, ATR Instrument. The NMR spectra were recorded in DMSO-d_6 solvent on Bruker Avance III 400 MHz NaNoBay FT-NMR spectrophotometer using tetramethyl silane as an internal standard.

The X-ray diffraction data was recorded on a Bruker APEX-II CCD diffractometer. A suitable crystal was selected and coated with Paratone oil and mounted onto a Nylon loop on a Bruker APEX-II CCD diffractometer. The crystal was kept at T = 100 K during data collection. The data were collected with MoKα (λ = 0.71073 Å) radiation at a crystal-to-detector distance of 40 mm. Using Olex2 [30], the structure was solved with the Superflip [31-33] structure solution program, using the Charge Flipping solution method and refined by full-matrix least-squares techniques on F^2 using ShelXL [34] with refinement of F^2 against all reflections. Hydrogen atoms were constrained by difference maps and were refined isotropically, and all non-hydrogen atoms were refined anisotropically. The molecular structure plots were prepared using PLATON [33]. The geometric special details: all e.s.d.'s (except the e.s.d. in the dihedral angle between two l.s. planes) are estimated using the full covariance matrix. The cell e.s.d.'s are taken into account individually in the estimation of e.s.d.'s in distances, angles and torsion angles; correlations between e.s.d.'s in cell parameters are only used when they are defined by crystal symmetry. An approximate (isotropic) treatment of cell e.s.d.'s is used for estimating e.s.d.'s involving l.s. planes.

2.2. Synthesis and characterization

2.2.1. Synthesis of N-(dibenzylcarbamothioyl)-3-methyl butanamide

A solution of 3-methylbutanoyl chloride (5×10^{-2} mol) in dry acetone (50 mL) was added dropwise to a suspension of potassium thiocyanate (5×10^{-2} mol) in acetone (30 mL). The reaction mixture was heated under reflux for 30 min, and then cooled to room temperature. A solution of dibenzylamine (5×10^{-2} mol) in acetone (10 mL) was added and the resulting mixture was stirred for 2 h. After, the reaction mixture was poured into hydrochloric acid (0.1 N, 300 mL), and the solution filtered [35]. The solid product was washed with water and purified by recrystallization from an ethanol: dichloromethane mixture (5:1, *v*:*v*) (Scheme 1). FT-IR (ATR, ν, cm^{-1}): 3272 (NH), 3030 (Ar-CH), 1688 (C=O), 1589 (C=C), 1189 (C=S). ^{1}H NMR (400 MHz, DMSO-d_6, ppm): 10.57 (s, 1H, NH), 7.37-7.14 (m, 10H, Ar-H), 5.14 (s, 2H, CH_2), 4.62 (s, 2H, CH_2), 2.18 (d, 2H, J = 8 Hz, CH_2), 2.04 (m, 1H, CH), 0.88 (d, 6H, J = 8 Hz, CH_3). ^{13}C NMR (100 MHz, DMSO-d_6, ppm): 183.46 (C=S), 164.51 (C=O), 135.79 (Ar-C), 132.75 (Ar-C), 132.40 (Ar-C), 128.72 (Ar-C), 128.47 (Ar-C), 128.39 (Ar-C), 127.42 (Ar-C), 55.56 (C-N), 54.07 (C-N), 46.1 (CH_2), 27.6 (CH), 22.2 (CH_3).

2.3. Hirshfeld surfaces analysis

Analysis of Hirshfeld surfaces and their associated two-dimensional fingerprint plots of the title compound were calculated using CrystalExplorer 17 [36]. The Hirshfeld surfaces mapped with different properties d_{norm}, shape index, curvedness. The d_{norm} is normalized contact distance, defined in terms of d_e, d_i and the vdW radii of the atoms. Deformation density is generated from CrystalExplorer 17, over the electron density isosurface (the value is 0.008 e/au^3) using HF method with 6-31G(d) as basis set.

2.4. Antimicrobial activity studies

Antimicrobial susceptibility testing was performed by modification microdilution of the following literature methods [37,38]. We used microbial strains such as *Staphylococcus aureus* (ATCC 25923), *Streptococcus pneumonia* (ATCC 6303), *Escherichia coli* (ATCC 35218), *Pseudomonas aeruginosa* (ATCC 27853), *Acinetobacter baumannii* (RSHM 2026), *Candida albicans* (ATCC 10231) and *Candida glabrata* (RSHM 40199).

The fungal and bacterial cell inoculums were prepared from the stock culture grown in Tryptic Soy Agar (TSA) at 28 °C for 24 h and Mueller-Hinton Agar (MHA) 37 °C for 24 h, respectively. The microorganism suspension concentrations were adjusted according to McFarland 0.5 turbidity tubes using sterilized saline. Stock solution of title compound was prepared in DMSO at 1000 µg/mL. A modified microdilution test was applied for antimicrobial activity and the experiments were run in duplicates independently. For antifungal activity testing, 100 µL Tryptic Soy Broth (TSB) was added to each of 11 wells. 100 µL of chemical derivative solution was added to the first well and 2-fold dilutions were prepared. Then, 5 µL of fungal suspension was added to each tube except the last one which acted control well.

For antibacterial activity testing, 100 µL Mueller-Hinton Broth (MHB) was added to each of 11 well. 100 µL of chemical derivative solution was added to the first tube and 2-fold dilutions were prepared. Then, 5 µL of the bacterial suspension was added to each tube except the last control well. Only 5 µL of fungal and bacterial suspension were added in another to control tube without chemical and used as control for growing. All plate were incubated at 28 °C (for fungi) and at 37 °C (for bacteria) for 24 h. After the incubation, the minimal inhibitory concentrations (MIC) were noted by controlling the growth inhibition for title compound.

Table 1. Crystal data and details of the structure refinement for title compound.

Parameters	Compound
Empirical formula	$C_{20}H_{24}N_2OS$
Formula weight	340.47
Temperature (K)	107.18
Crystal system	Monoclinic
Space group	C2/c
a (Å)	19.6882(9)
b (Å)	9.4045(4)
c (Å)	19.5012(8)
β (°)	98.433(2)
Volume (Å^3)	3571.8(3)
Z	8
ρ_{calc} (g/cm^3)	1.266
μ (mm^{-1})	1.665
F(000)	1456.0
Crystal size (mm^3)	0.42 × 0.36 × 0.24
Radiation	CuKα (λ = 1.54178)
2Θ range for data collection (°)	9.168 to 144.196
Index ranges	$-24 \le h \le 20$, $-11 \le k \le 11$, $-23 \le l \le 24$
Reflections collected	25057
Independent reflections	3500 [R_{int} = 0.0322, R_{sigma} = 0.0200]
Data/restraints/parameters	3500/0/219
Goodness-of-fit on F^2	1.074
Final R indexes [I≥2σ (I)]	R_1 = 0.0363, wR_2 = 0.0900
Final R indexes [all data]	R_1 = 0.0377, wR_2 = 0.0910
Largest diff. peak/hole (e Å^{-3})	0.58/-0.64

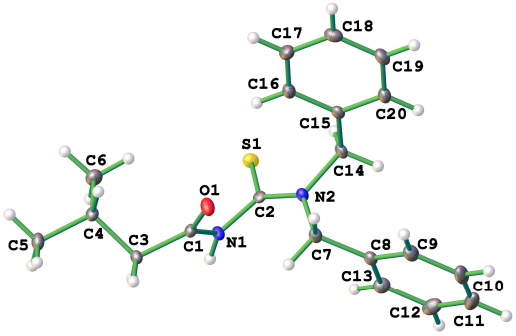

Figure 1. Molecular structure of the title compound showing the atom-numbering scheme

Fluconazole and ampicillin were used as reference drugs. The results were read visually and by measuring optical density for 24 h.

3. Result and discussion

3.1. Spectral characterization

The title compound was synthesized according to the general method early reported by Douglass and Dains [35]. The synthesis procedure of the title compound involves the *in situ* reaction between 3-methylbutanoyl chloride and KSCN and the reaction of the intermediate 3-methylbutanoyl isothiocyanate with dibenzylamine. The reaction proceeds *via* a nucleophilic addition of the amine to the isothiocyanate with good yields. The synthesized compound was purified by recrystallization from an dichloromethane:ethanol mixture and characterized by ^{1}H NMR, ^{13}C NMR and FT-IR spectroscopy.

The title compound **1** shows characteristic peaks in FT-IR due to ν(N-H) and ν(C=O) groups stretching vibration at 3272 and 1688 cm^{-1}, respectively. Also, the band at 3030 cm^{-1} corresponds to stretching of ν(C_{sp^2}-H) groups of the title compound. Intense absorptions in the 1500-1600 cm^{-1} region due to the δ(N-H) deformation modes are usually observed in the infrared spectra of thioureas [39].

In ^{1}H NMR, the title exhibited broad signal at the δ 10.98 ppm which was assigned to the N-H proton. The signals for the aromatic protons in the compound **1** were observed in the range of δ 7.49-7.31 ppm. Also, the peak at δ 2.40 ppm seen as multiplet in ^{1}H NMR spectrum correspond to CH group while the peak at δ 0.98 ppm seen as triplet correspond to CH_3 groups. ^{13}C NMR spectrum showed the peaks at about δ 183.46 for C=S and 164.51 ppm for C=O, respectively.

3.2. Crystal structure analysis

Good quality single crystals were obtained by slow evaporation of a dichloromethane:ethanol (1:5, *v*:*v*) solution. The crystal belongs to the monoclinic system with space group C2/*c*. The crystal data and structure refinement parameters are summarized in Table 1. Selected bond lengths and bond angles are given in Table 2. The asymmetric unit of the title complex along with an atom numbering scheme is shown in Figure 1.

The C=S and C=O bonds show a typical double bond character with bond lengths of 1.674 Å and 1.225 Å, respectively [40-46]. The C-N bond lengths for the title compound are shorter than a C-N single bond. This fact indicates that these bonds have a pronounced double bond character. In the compound, O=C-N-C the torsion angle is at the of 20.15°. The dihedral angles between the O-C-N and S-C-N planes of compound is 50.15°.

The molecular structure of title compound is stabilized by C-H···S (2.543 Å, ∠ 114 °) intramolecular hydrogen bonds (Table 3).

Table 2. Selected bond lengths (Å), bond and torsion angles (°) of title compound.

Atom		Length (Å)	Atom			Angle (°)	Atom				Angle (°)
S1	C2	1.6737(14)	C1	N1	C2	123.67(11)	O1	C1	C3	C4	67.75(16)
O1	C1	1.2246(17)	C2	N2	C7	124.54(11)	N1	C1	C3	C4	-109.27(13)
N1	C1	1.3829(17)	C2	N2	C14	120.75(11)	N2	C7	C8	C9	119.10(14)
N1	C2	1.4150(17)	C14	N2	C7	114.70(10)	N2	C7	C8	C13	-61.36(16)
N2	C2	1.3383(17)	O1	C1	N1	122.95(12)	N2	C14	C15	C16	-50.04(17)
N2	C7	1.4785(17)	O1	C1	C3	121.85(12)	N2	C14	C15	C20	133.69(13)
N2	C14	1.4708(16)	N1	C1	C3	115.14(11)	C1	N1	C2	S1	-120.17(12)
C1	C3	1.5060(18)	N1	C2	S1	117.65(10)	C1	N1	C2	N2	60.12(17)

Table 3. Intra- and inter-molecular hydrogen bonds for title compound (Å, °).

D-H···A	d(D-H)	d(H···A)	d(D···A)	∠(D-H···A)	Symmetry
C14-H14···S1	0.99	2.543	3.0763(5)	114	-
N1-H1···O1	0.88	2.26	3.0441(14)	148.7	1/2-*x*, 1/2+*y*, 1/2-*z*
C3-H3A···O1	0.99	2.40	3.3093(16)	152.0	1/2-*x*, 1/2+*y*, 1/2-*z*
C3-H3A···S1	0.99	2.84	3.7369(13)	151.5	1/2-*x*, -1/2+*y*,1/2-*z*

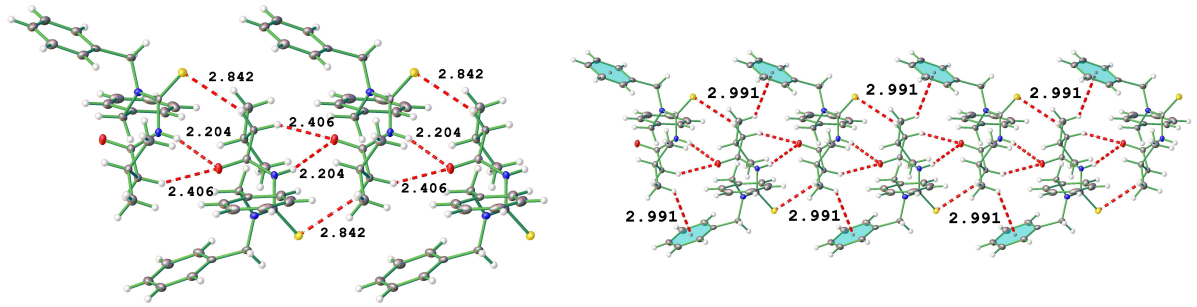

(**a**) (**b**)

Figure 2. (**a**) The intermolecular N-H···O, C-H···O and C-H···S hydrogen bonds, (**b**) The C-H···π stacking interactions formed along the *a*-axis.

The crystal structure of title compound is also dominated by intermolecular hydrogen bonds such as N-H···O, C-H···O, C-H···S that cause to form molecular pack (Figure 2a, Table 3). The H···O intermolecular interactions are generated by amide and CH_2 hydrogen atoms and the carbonyl group oxygen atom function as hydrogen bond acceptors, forcing the molecule to form two hydrogen bonds. Due to this, the molecule forms parallel chain to the *a*-axis. Similarly, the H···S intermolecular interactions occur between thiocarbonyl sulphur atom and CH_2 hydrogen atoms. So, molecules zig-zag chains along the *a*-axis inter-connected *via* the S···H contacts. The crystal lattice of the title compound is additionally supported by C–H···π interactions (2.991 Å, symmetry code: 3/2-*x*, -1/2+*y*, 3/2-*z*) formed bet-ween methyl groups and phenyl rings of dibenzyl amine part along the same axis (Figure 2b).

The sight of the crystal packing along the *b*-axis in the title compound reveals π···π interactions. In the crystal structure of the title compound, Cg(1) and Cg(2) are the centroids of the rings C8-C13 and C15-C20, respectively. Two adjacent molecules are connected together by the π···π stacking between the dibenzylamine rings with Cg(1)···Cg(2) distance of 4.736 Å with symmetry code: 1-*x*, 1-*y*, 1-*z* and 4.322 Å with symmetry code: 1-*x*, *y*, 3/2-*z*. These interactions infinitely repeated lead to a ladder-like chain running along *b*-direction (Figure 3, Table 4).

The presence of intermolecular hydrogen bonds, π···π and C–H···π stacking interactions in the title compound contribute to stabilize the crystal packing and account for the ease of obtaining single crystals for this compound, because it is a relatively strong bond type and thus has great influence on the supramolecular arrangement.

3.3. Hirshfeld surfaces analysis

Intermolecular contacts obtained from X-ray single crystal diffraction study were also explored using both Hirshfeld surfaces and fingerprint plots. Therefore, the intermolecular interactions in the crystal structure of the title compound have been examined *via* Hirshfeld surface analysis and fingerprint plots.

The Hirshfeld surfaces of the title compound have been mapped over a d_{norm} and shape index functions. All the Hirshfeld surfaces are shown as transparent to allow visualization of the title compound, around which they were calculated. Red-blue-white color scheme seen in the d_{norm} surface represent shorter contacts, longer contacts and equal contacts around the Van der Walls separation, respectively [47].

As can be seen in the Hirshfeld surfaces of the title compound, the most intense red regions occur near to C=O, N–H and CH_2 groups, due to N–H···O and C-H···O hydrogen bonds present in structure. Also, the weaker H···S=C contacts formed between C=S and CH_2 groups in the Hirshfeld surface mapped over d_{norm} give rise to visible as weak red spots. Figure 4 displays the Hirshfeld surface of title compound mapped over d_{norm} in front and back views and d_{norm} Hirshfeld surface surrounded by one neighboring molecule associated with close contacts. When we look at Hirshfeld surface of the title compound, it is observed that except the H···O and H···S interactions, is not involved in any close intermolecular contact, resulting in a white-to-blue gradient color in the Hirshfeld surface.

The analysis about C···H interactions of the title compound was done using the Hirshfeld surface shape index (Figure 5). C···H/H···C interactions are mainly responsible for the molecular packing in the supramolecular structure and represent C-H···π interactions. These interactions on the Hirshfeld surface mapped with shape index function are appearing as hollow orange areas (π···H-C) and bulging blue areas (C-H···π).

The 2D fingerprint plots obtained from the Hirshfeld surface analysis illustrate the percentage contributions of intermolecular interactions on the molecules [48,49]. 2D fingerprint plots are mainly responsible for crystal packing of solid networks of the compound.

Table 4. Geometrical parameters of π···π interactions for title compound (Å, °).

Rings I–J [a]	Cg(I)···Cg(J) [b]	γ [c]	Cg(I)-perp [d]	Cg(J)-perp [e]	Symmetry
Cg(1)···Cg(2)	4.7359(8)	49.4	-3.0845(5)	-3.6763(5)	1-*x*, 1-*y*, 1-*z*
Cg(2)···Cg(1)	5.7814(8)	64.5	2.4883(5)	-3.1475(5)	*x*, *y*, *z*
Cg(2)···Cg(1)	4.7359(8)	39.1	-3.6762(5)	-3.0845(5)	1-*x*, 1-*y*, 1-*z*
Cg(2)···Cg(2)	4.3217(8)	35.4	3.5211(5)	3.5211(5)	1-*x*, *y*, 3/2-*z*

[a] Cg(1) and Cg(2) are the centroids of the rings C8-C13 and C15–C20 for the title compound, respectively.
[b] Centroid distance between ring I and ring J.
[c] Angle between the centroid vector Cg(I)···Cg(J) and the normal to plane J.
[d] Perpendicular distance of Cg(I) on ring J (Å).
[e] Perpendicular distance of Cg(J) on ring I (Å).

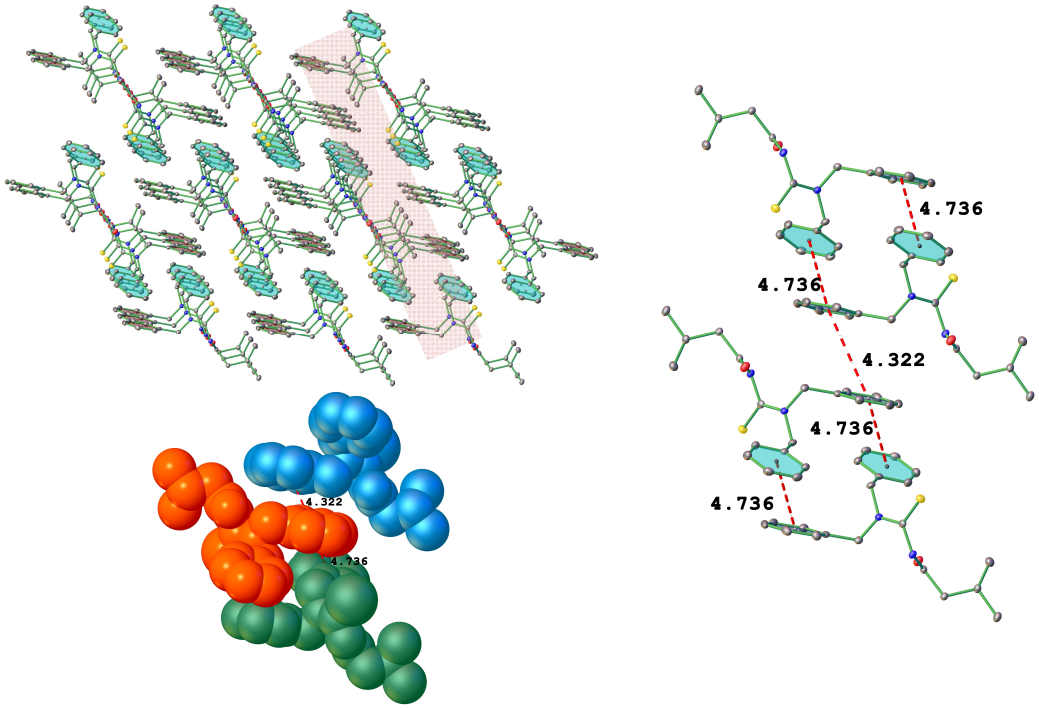

Figure 3. The intermolecular π···π stacking interactions form infinitely repeated a ladder-like chain running along b-direction.

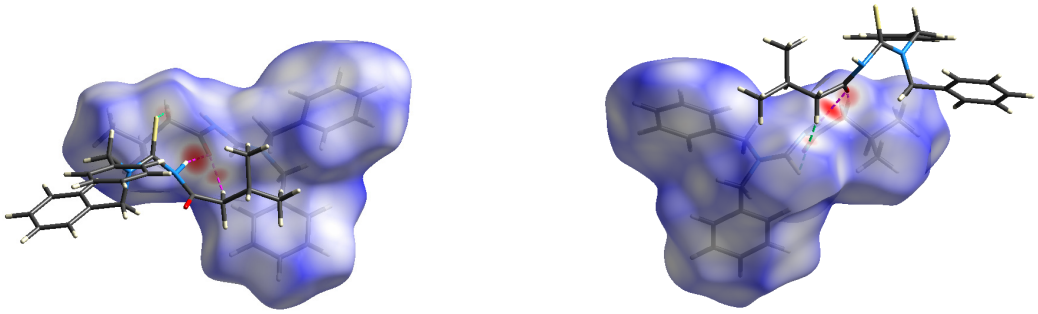

Figure 4. The Hirshfeld surface of the title compound mapped over d_{norm} (front and back) and d_{norm} Hirshfeld surface surrounded by one neighboring molecule associated with close contacts.

Moreover, these plots can be decomposed to quantify particular contributions of intermolecular interactions in the molecular packing of a solid network. Also, the fingerprint plots indicate a molecule act as a donor ($d_e > d_i$) and another one is found as an acceptor ($d_e < d_i$). This analysis show that the contributions to the total Hirshfeld surface of H···H, C···H, O···H and S···H including reciprocal contacts for the title compound is observed as 64.0, 19.1, 4.9 and 10.0%, respectively (Figure 6).

The 3D electrostatic potential and deformation density maps of the title compound were generated from the CrystalExplorer 17 [36], (isosurface 0.05 au for electrostatic potential and isosurface 0.008 au for deformation density) using HF method with 6-31G(d) as basis set.

Figure 7a displays the isosurface representation electrostatic potential surface of the title compound. The electrostatic potential map shows that a large electropositive region is around the dibenzylamine rings and a large electronegative region is at the vicinity of the thiocarbonyl and on carbonyl oxygen atom. The positive electrostatic potential surface (blue) around the dibenzylamine ring occurs because of the positive charge contribution of C atoms of the ring.

Table 5. MIC values (μg/mL) of the title compound tested against the Gram positive, Gram negative bacteria and fungal.

Compound	Gram positive bacteria			Gram negative bacteria			Fungi	
	S. Aureus	***S. Pneumoniae***	***B. Subtilis***	***E. Coli***	***P. Aeruginosa***	***A. Baumannii***	***C. Albicans***	***C. Glabrata***
Title compound	62.5	62.5	62.5	62.5	62.5	31.25	31.25	31.25
Flucanozole							*	*
Ampicillin	*	*	*	31.25	*	15.62		

"*": Effective in all concentrations used.

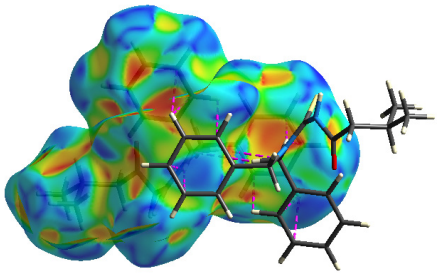

Figure 5. The Hirshfeld surface mapped over the shape index with C-H···π interactions between two vicinal molecules of title compound.

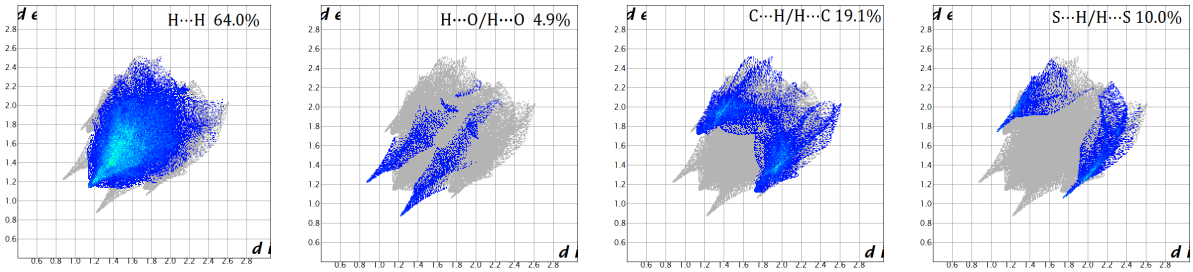

Figure 6. 2D fingerprint plots for interactions present in the title compound.

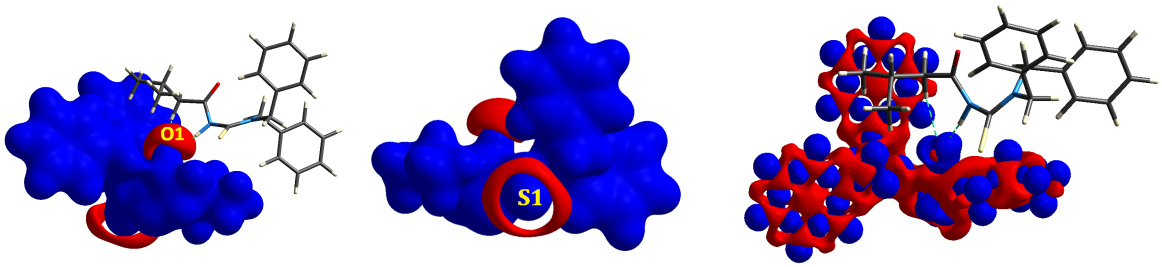

(**a**) (**b**)

Figure 7. (**a**) Electrostatic potential mapped on Hirshfeld surface (different orientation) with 0.05 au. Blue region corresponds to positive electrostatic potential and red region to negative electrostatic potential, (**b**) 3D-deformation density map of the title compound with 0.008 au.

The O1 atom also exhibits a high negative electrostatic potential region. This atom forms hydrogen-bonding interactions with the NH and CH_2 groups of the title compound.

A 3D-deformation density map showing the presence of CD regions (in red) and CC regions (in blue) on the title compound, is also mapped by CrystalExplorer 17 [36]. The deformation density represents differences between the total electron density of a molecule and the electron density of "neutral spherical unperturbed atoms" superimposed in the same of the molecule [50,51]. The electrostatic deformation density map reveals the presence of a charge depletion region (in red) at the hydrogen atoms (hydrogen atoms H1/H14 of NH and CH_2 groups) which is directed towards the charge concentration region (in blue) over oxygen atom, facilitating formation of the H···O contacts in the crystal. In Figure 7b, the green dashed line indicates the intramolecular H···O interaction. The charge depletion and charge concentration regions in the H···O contact provide the overall stabilization in complex structure.

3.4. Antimicrobial activity studies

The *in vitro* biological activity of the title compound was tested towards six Gram positive/negative bacteria and two types of fungal. The organisms used in the present investigations included *S. Aureus*, *B. Subtilis* and *S. pneumoniae* (as Gram positive bacteria), *E. coli*, *P. aeruginosa* and *A. baumannii* (as Gram negative bacteria) and *C. albicans* and *C. glabrata* (as fungal). The results of the biological activity of the title compound are compared with fluconazole (for fungal) and ampicillin (for bacteria) reference drugs. The obtained MIC values are listed in Table 5.

According to data generated from this study, the title compound showed moderate inhibitory action against bacteria

strains with MIC values ranging between 31.25-62.5 µg/mL and exhibited the highest activities against *A. baumannii* bacterium with MIC values at 31.25 µg/mL. But when the title compound was compared with ampicillin used as reference drug, it demonstrated lower activity against all the bacteria chains. The title compound inhibited the growth of fungal strains with MIC values at 31.25 µg/mL but it isn't as effective as fluconazole used as reference drug against all fungal strains. Hence, from all these observations, it was concluded that the title compound could not be exploited for the design of novel antimicrobial drug.

4. Conclusion

In this study, *N*-(dibenzylcarbamothioyl)-3-methylbutanamide as a thiourea derivative was synthesized and structurally characterized by NMR and FT-IR spectroscopic techniques. The molecular structure of the prepared compound was also characterized by the single crystal X-ray diffraction method. In the title compound, the intermolecular contacts have been also examined based on the Hirshfeld surfaces and their associated 2D fingerprint plots. Furthermore, the title compound was evaluated for both, their *in-vitro* antibacterial and antifungal activity.

Acknowledgement

This work was supported by Mersin University Research Fund [Project No: 2016-AP4-1426]. This academic work was linguistically supported by the Mersin Technology Transfer Office Academic Writing Center of Mersin University.

Supplementary material

Crystallographic data for the structure reported in this paper have been deposited at the Cambridge Crystallographic Data Centre (CCDC) with quotation number CCDC-1581128 for *N*-(dibenzylcarbamothioyl)-3-methylbutanamide and can be obtained free of charge on application to CCDC 12 Union Road, Cambridge CB2 1EZ, UK [Fax: (internat.) +44(1223)336-033, E-mail: deposit@ccdc.cam.ac.uk].

References

[1]. Mushtaque, M.; Jahan, M.; Ali, M.; M. S. Khan; Khan, M. S.; Sahay, P.; Kesarwani, A. *J. Mol. Struc.* **2016**, *1122*, 164-174.
[2]. Kodomari, M.; Suzuki, M.; Tanigawa, K.; Aoyama, T. *Tetrahedron Lett.* **2005**, *46,* 5841-5843.
[3]. Lesyk, R.; Zimenkovsky, B.; Curr. *Org. Chem.* **2004**, *8*, 1547-1577.
[4]. Lesyk, R.; Vladzimirska, O.; Holota, S.; Zaprutko, L.; Gzella, A. *Eur. J. Med. Chem*. **2007**, *42*, 641-648.
[5]. Havrylyuk, D.; Zimenkovsky, B.; Vasylenko, O.; Zaprutko, L.; Gzella, A.; Lesyk, R. *Eur. J. Med. Chem.* **2009**, *44,* 1396-1404.
[6]. Mushtaque, M.; Avecilla, F.; Khan, M. S.; Hafeez, Z. B.; Rezvi, M. M. A.; Srivastava, A. *J. Mol. Struc.* **2017**, *1141*, 119-132.
[7]. Gomes, L. R.; Santos, L. M. N. B. F.; Coutinho, J. A. P.; Schroder, B.; Low, J. N. *Acta Crystallogr. E* **2010**, *66*, o870-o870.
[8]. Saeed, A.; Florke, U. *Acta Crystallogr. E* **2006**, *62*, o2403-o2405.
[9]. Janiak, C. J. *Chem. Soc. Dalton Trans*. **2000**, 3885-3896.
[10]. Seth, S. K.; Manna, P.; Singh, N. J.; Mitra, M.; Jana, A. D.; Das, A.; Choudhury, S. R.; Kar, T.; Mukhopadhyay S.; Kim, K. S. *Cryst. Eng. Comm.* **2013**, *15*, 1285-1288.
[11]. Habtu, M. M.; Bourne, S. A.; Koch, K. R.; Luckay, R. C. *New J. Chem.* **2006**, *30*, 155-162.
[12]. Saeed, A.; Bolte, M.; Erben, M. F.; Perez, H. *Cryst. Eng. Comm.* **2015**, *17*, 7551-7563.
[13]. Weiqun, Z.; Wen, Y.; Liqun, X.; Xianchen, C. *J. Inorg. Biochem.* **2005**, *99*, 1314-1319.
[14]. Yang, W.; Liu, H.; Li, M.; Wang, F.; Zhou, W.; Fan, J. *J. Inorg. Biochem.* **2012**, *116*, 97-105.
[15]. Selvakumaran, N.; Pratheepkumar, A.; Ng, S. W.; Tiekink, E. R. T.; Karvembu, R. *Inorg. Chim. Acta* **2013**, *404*, 82-87.
[16]. Yesilkaynak, T.; Binzet, G.; Emen, F. M.; Florke, U.; Kulcu, N.; Arslan, H. *Eur. J. Chem.* **2010**, *1(1)*, 1-5.
[17]. Saeed, A.; Mumtaz, A.; Florke, U. *Eur. J. Chem.* **2010**, *1(2)*, 73-75.
[18]. Gumus, I.; Solmaz, U.; Celik, O.; Binzet, G.; Balci, K. G.; Arslan, H. *Eur. J. Chem.* **2015**, *6(3)*, 237-241.
[19]. Saeed, S.; Rashid, N.; Jones, P.; Hussain, R. *Eur. J. Chem.* **2011**, *2(1)*, 77-82.
[20]. Saeed, S.; Rashid, N.; Ali, M.; Hussain, R.; Jones, G. P. *Eur. J. Chem.* **2010**, *1(3)*, 221-227.
[21]. Binzet, G.; Florke, U.; Kulcu, N.; Arslan, H. *Eur. J. Chem.* **2012**, *3(1)*, 37-39.
[22]. Binzet, G.; Florke, U.; Kulcu, N.; Arslan, H. *Eur. J. Chem.* **2012**, *3(2)*, 211-213.
[23]. Egan, T. J.; Koch, K. R.; Swan, P. L.; Clarkson, C.; Van Schalkwyk, D. A.; Smith, P. J. *J. Med. Chem.* **2004**, *47*, 2926-2934.
[24]. Gunasekaran, N.; Bhuvanesh, N. S. P.; Karvembu, R. *Polyhedron* **2017**, *122*, 39-45.
[25]. Ferreira, F. F.; Trindade, A. C.; Antonio, S. G.; De Oliveira Paiva-Santos, C. *Cryst. Eng. Comm.* **2011**, *13*, 5474-5479.
[26]. Yamin, B. M.; Osman, U. M. *Acta Crystallogr. E* **2011**, *67*, o1286-o1286.
[27]. Zhu, W.; Yang, W.; Zhou, W.; Liu, H.; Wei, S.; Fan, J. *J. Mol. Struct.* **2011**, *1004*, 74-81.
[28]. Sun, J.; Cai, S.; Mei, H.; Li, J.; Yan, N.; Wang, Q.; Lin, Z.; Huo, D. *Chem. Biol. Drug Des.* **2010**, *76(3)*, 245-254.
[29]. Saeed, A.; Khurshid, A.; Bolte, M.; Fantoni, A. C.; Erben, M. F. *Spectrochim. Acta A* **2015**, *143*, 59-66.
[30]. Dolomanov, O. V.; Bourhis, L. J.; Gildea, R. J.; Howard, J. A. K.; Puschmann, H. *J. Appl. Cryst.* **2009**, *42*, 339-341.
[31]. Palatinus, L.; Chapuis, G. *J. Appl. Cryst.* **2007**, *40*, 786-790.
[32]. Palatinus, L.; van der Lee, A. *J. Appl. Cryst.* **2008**, *41*, 975-984.
[33]. Palatinus, L.; Prathapa, S. J.; van Smaalen, S. *J. Appl. Cryst.* **2012**, *45*, 575-580.
[34]. Sheldrick, G. M. *Acta Crystallogr. C* **2015**, *71*, 3-8.
[35]. Douglass, I. B.; Dains, F. B. *J. Am. Chem. Soc.* **1934**, *56*, 719-721.
[36]. Turner, M. J.; McKinnon, J. J.; Wolff, S. K.; Grimwood, D. J.; Spackman, P. R.; Jayatilaka, D.; Spackman, M. A. CrystalExplorer 17, University of Western Australia, 2017.
[37]. Burlesson, F. G.; Chambers, T. M.; Wedbrauk, D. L. Virology. A Laboratory Manual, Academic Press, New York, 1992.
[38]. National Committee for Clinical Laboratory Standards. Reference method for broth dilution antifungal susceptibility testing of yeasts. Approved standard NCCLS document M27-A. National Committee for Clinical Laboratory Standards, Wayne, Pa., 2002.
[39]. Yusof, M. S. M.; Jusoh, R. H.; Khairul, W. M.; Yamin, B. M. *J. Mol. Struct.* **2010**, *975*, 280-284
[40]. Rauf, M. K.; Ebihara, M.; Badshah, A. *Acta Crystallogr. E* **2012**, *68*, o119-o119.
[41]. Yang, W.; Zhou, W. Q.; Zhang, Z. J. *J. Mol. Struct.* **2007**, *828*, 46-53.
[42]. Arslan, H.; Florke, U.; Kulcu, N.; Binzet, G. *Spectrochim. Acta A* **2007**, *68*, 1347-1355.
[43]. Yusof, M. S.; Jusoh, R. H.; Khairul, W. M.; Bohari, M. Y. *J. Mol. Struct.* **2010**, *975*, 280-284.
[44]. Al-Abbasi, A. A.; Yamin, B. M.; Kassim, M. B. *Acta Crystallogr. E* **2011**, *67*, 1891-1894.
[45]. Mohamadou, A.; Dechamps-Olivier, I.; Barbier, J. P. *Polyhedron* **1994**, *13*, 1363-1370.
[46]. Arslan, H.; Florke, U.; Kulcu. N. *Acta Chim. Slov.* **2004**, *51*, 787-792.
[47]. Spackman, M. A.; Jayatilaka, D. *Cryst. Eng. Comm*. **2009**, *11*, 19-32.
[48]. Spackman, M. A.; McKinnon, J. J. *Cryst. Eng. Comm*. **2002**, *4*, 378-392.
[49]. McKinnon, J. J.; Jayatilaka, D.; Spackman, M. A. *Chem. Commun.* **2007**, *37*, 3814-3816
[50]. Angeloski, A.; Hook, J. M.; Bhadbhade, M.; Baker, A. T.; McDonagh, A. M. *Cryst. Eng. Comm*. **2016**, *18*, 7070-7077.
[51]. Sarkar, S.; Pavan, M. S.; Row, T. N. G. *Phys. Chem. Chem. Phys.* **2015**, *17*, 2330-2334.